Structure, Volume *29*

Supplemental Information

Near-physiological-temperature serial crystallography reveals conformations of SARS-CoV-2 main protease active site for improved drug repurposing

Serdar Durdagi, Çağdaş Dağ, Berna Dogan, Merve Yigin, Timucin Avsar, Cengizhan Buyukdag, Ismail Erol, Fatma Betul Ertem, Seyma Calis, Gunseli Yildirim, Muge D. Orhan, Omur Guven, Busecan Aksoydan, Ebru Destan, Kader Sahin, Sabri O. Besler, Lalehan Oktay, Alaleh Shafiei, İlayda Tolu, Esra Ayan, Busra Yuksel, Ayse B. Peksen, Oktay Gocenler, Ali D. Yucel, Ozgur Can, Serena Ozabrahamyan, Alpsu Olkan, Ece Erdemoglu, Fulya Aksit, Gokhan Tanisali, Oleksandr M. Yefanov, Anton Barty, Alexandra Tolstikova, Gihan K. Ketawala, Sabine Botha, E. Han Dao, Brandon Hayes, Mengning Liang, Matthew H. Seaberg, Mark S. Hunter, Alex Batyuk, Valerio Mariani, Zhen Su, Frederic Poitevin, Chun Hong Yoon, Christopher Kupitz, Raymond G. Sierra, Edward H. Snell, and Hasan DeMirci

Supplementary Figures

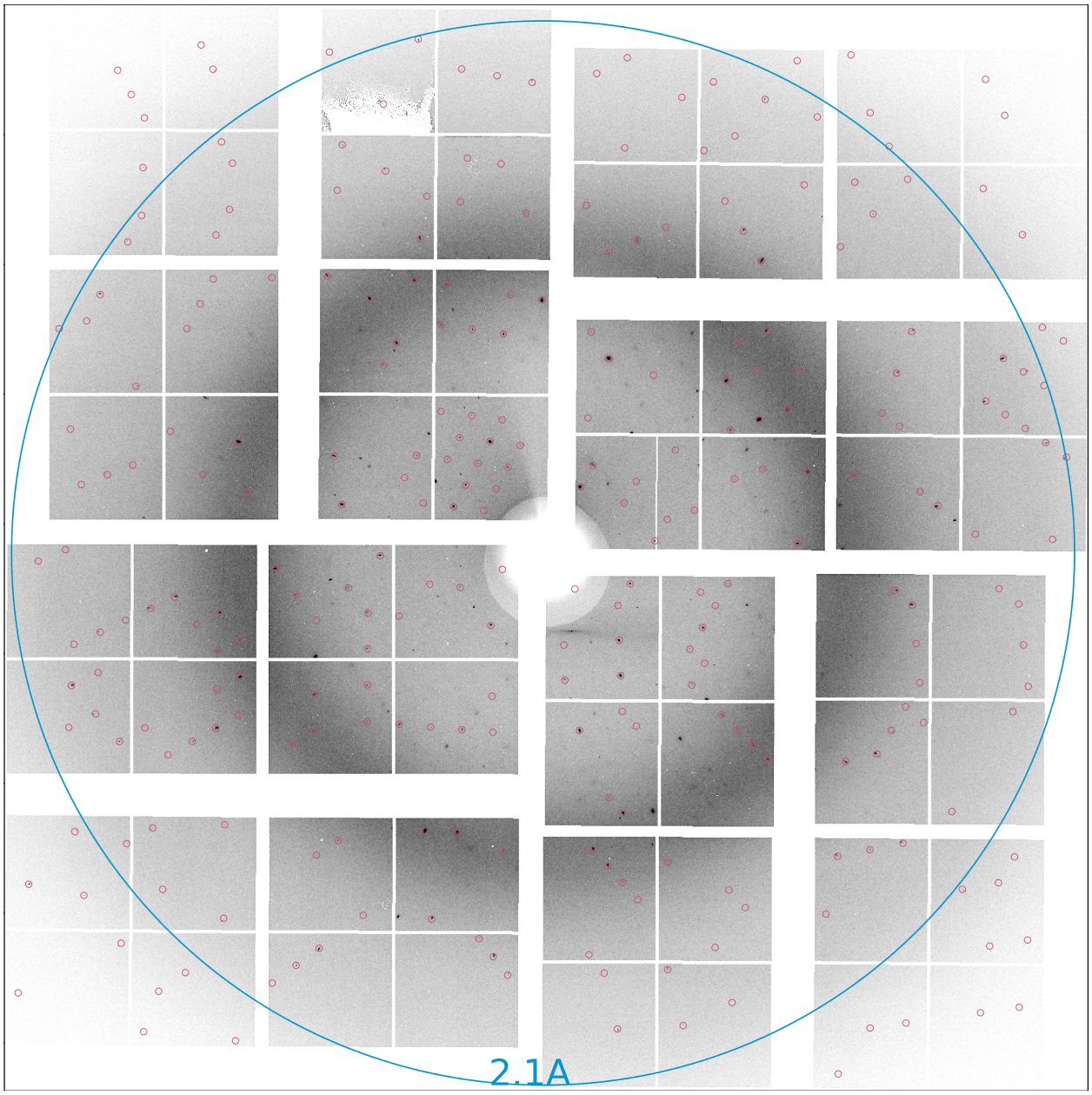

Figure S1 A diffraction pattern of monoclinic crystal form. Related to Figure 1.

A diffraction pattern of monoclinic crystal form in space group C121 (PDB ID: 7CWB) with indexed spots. The ePix10k2M detector has a non-functional panel (third panel from the top left) which was masked during data processing.

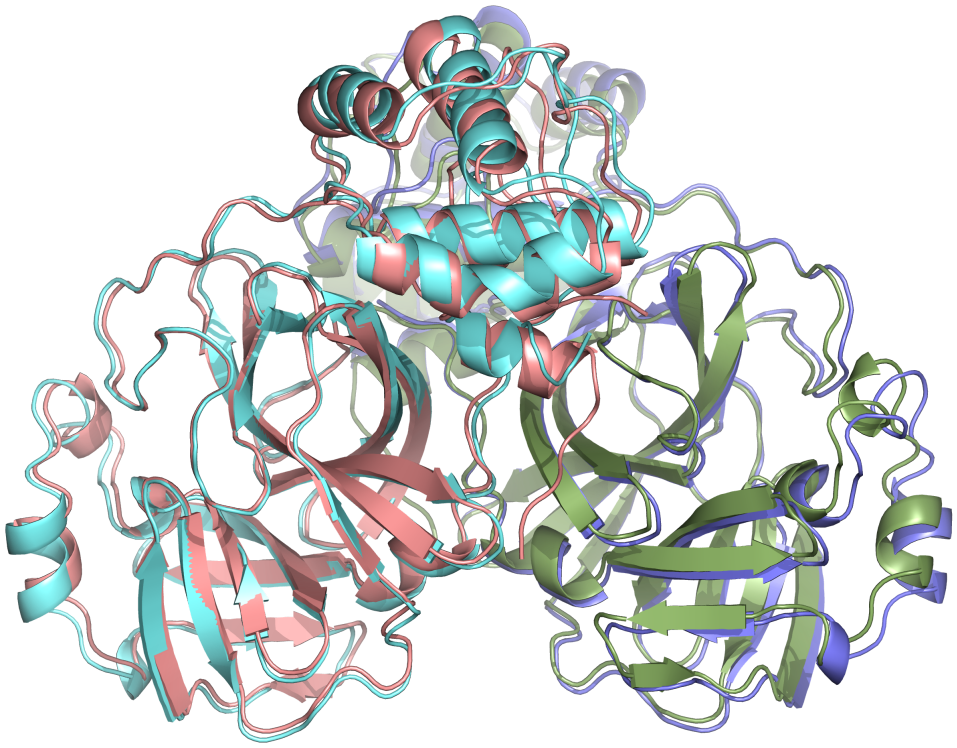

Figure S2 Superposition of two crystal forms. Related to Figure 1.

Native Mpro in space group C121 colored in dark-salmon and its symmetry mate in green. Modified Mpro in space group $P2_12_12_1$ is colored in pale-cyan and light blue. Two crystal structures align with an overall RMSD of 1.00 Å.

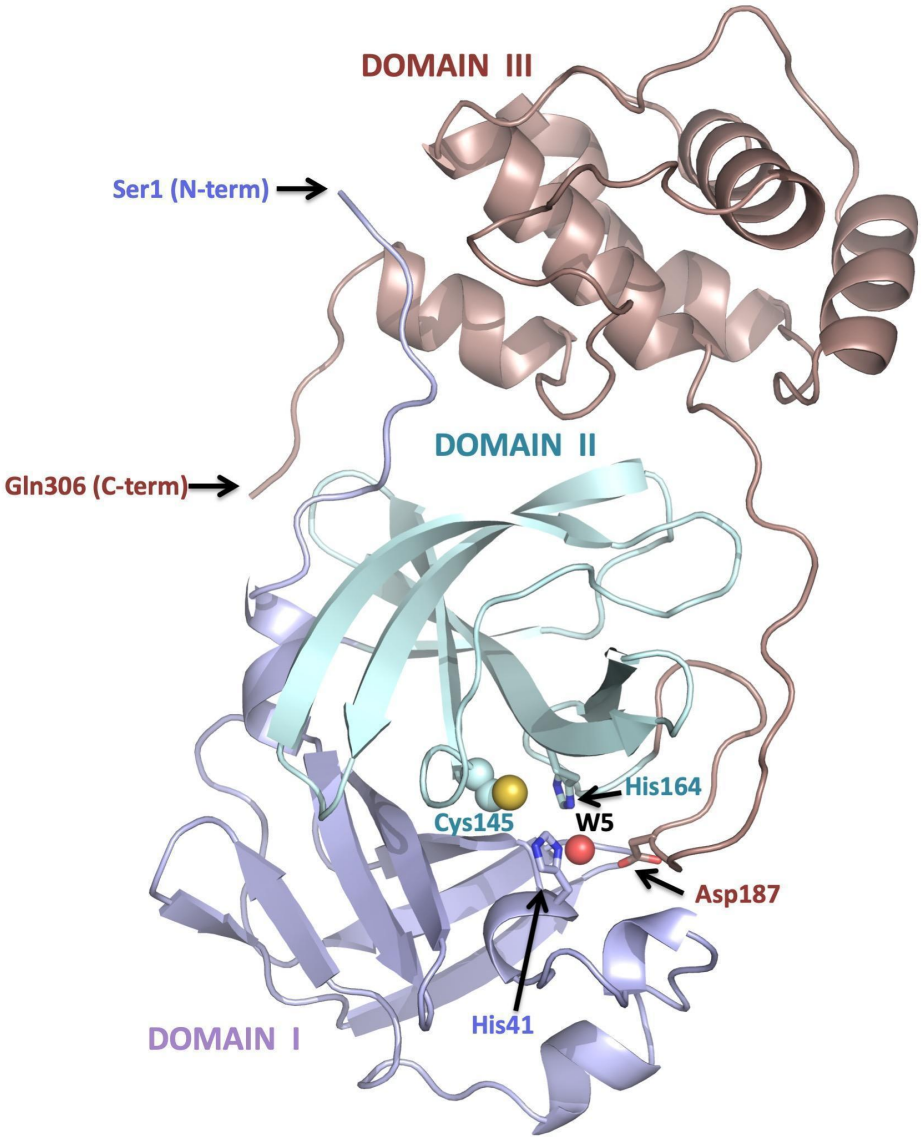

Figure S3 Three major domains of SARS-CoV-2 Mpro. Related to Figure 1.

Domain I is colored in light blue, domain II is colored in pale cyan and domain III is colored in dark salmon. Active site formed by residues from all three subdomains such as critical Cys145 are shown as spheres, His41, His164 and Asp187 shown in sticks. Red sphere labeled as W5 represents the water molecule in the binding pocket.

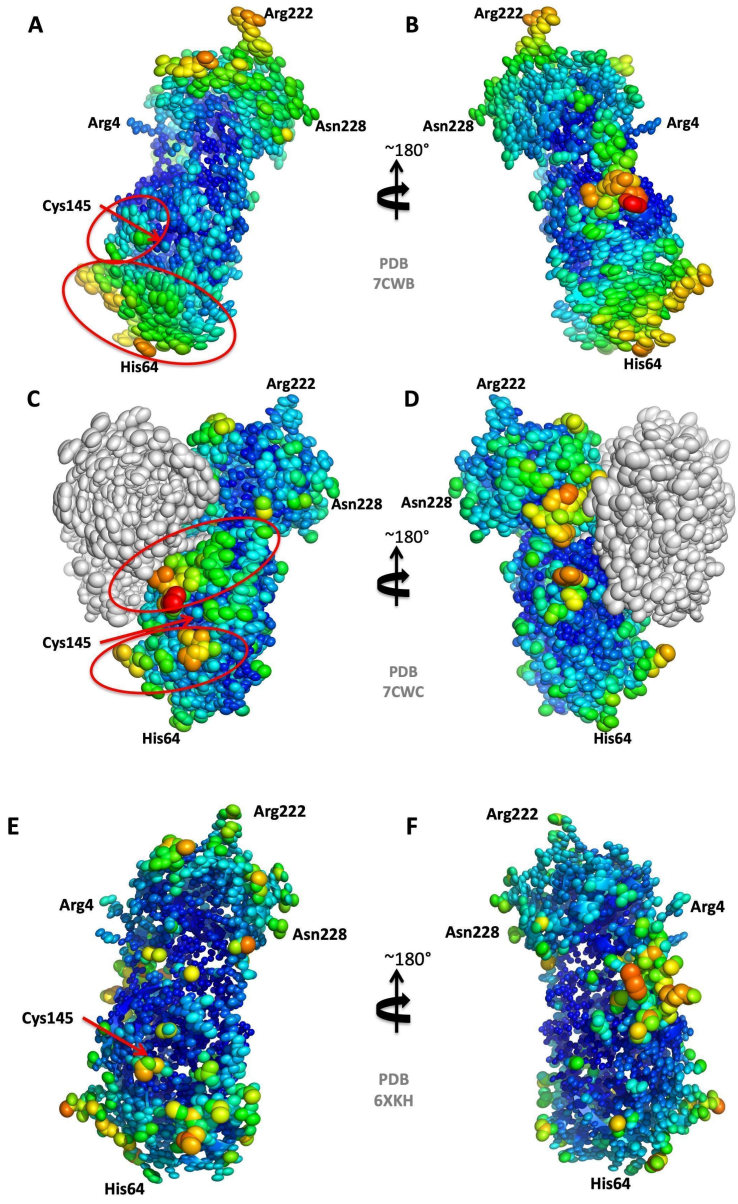

Figure S4 Representation of ellipsoids for SFX and cryogenic apo Mpro crystal structures (PDB IDs: 7CWB, 7CWC and 6XKH) based on B-factor. Related to Figure 6.

A) Mpro structure in space group C121 at 1.9 Å is examined to indicate the magnitude of thermal vibration. **B)** The 180 degrees rotated view of panel a) around y axis **C)** The dimer crystal form of Mpro structure in space group $P2_12_12_1$ at 2.1 Å is examined and chain A is colored by rainbow selection while chain B is colored by grey. **D)** The 180 degrees rotated panel c) around y axis. **E)** Mpro structure at 1.28 Å (PDB ID: 6XKH) is examined to compare our ambient-temperature crystal structures with the X-ray structure at 100 K. **F)** The 180 degrees rotated view of panel a) around y axis**.** All the ellipsoid structures are produced with *PyMOL* (www.pymol.org).

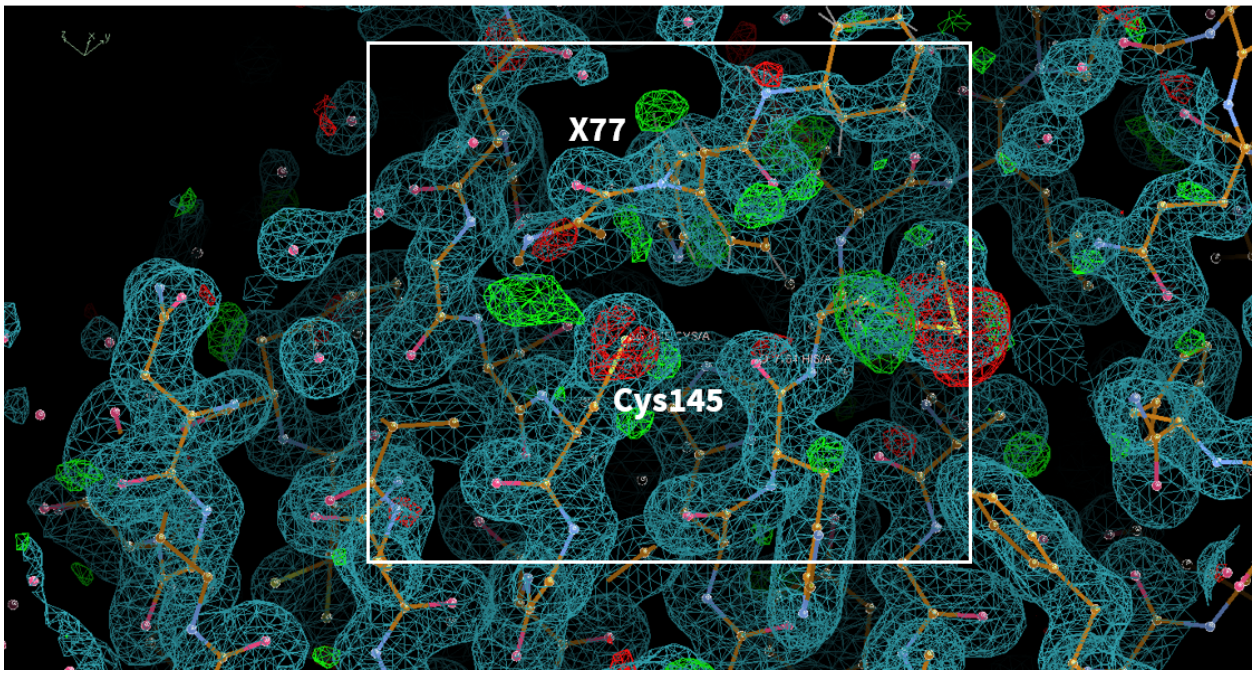

Figure S5 Representation of the 2Fo-Fc electron density map of SARS-CoV main protease (PDB ID: 6W79). Related to Figure 5.

Previously published structures are analysed to compare the non-covalent and covalent inhibitors of SARS-CoV main protease. Within them, SARS-CoV main protease complex with non-covalent inhibitor X77 is represented in the figure 5. In total 37 structures are analysed to reveal the mode of interaction between SARS-CoV main protease and its known inhibitors (Check the link for the detailed information: https://kuybim.ku.edu.tr/wp-content/uploads/2021/07/Supplementary_Figures.pdf)

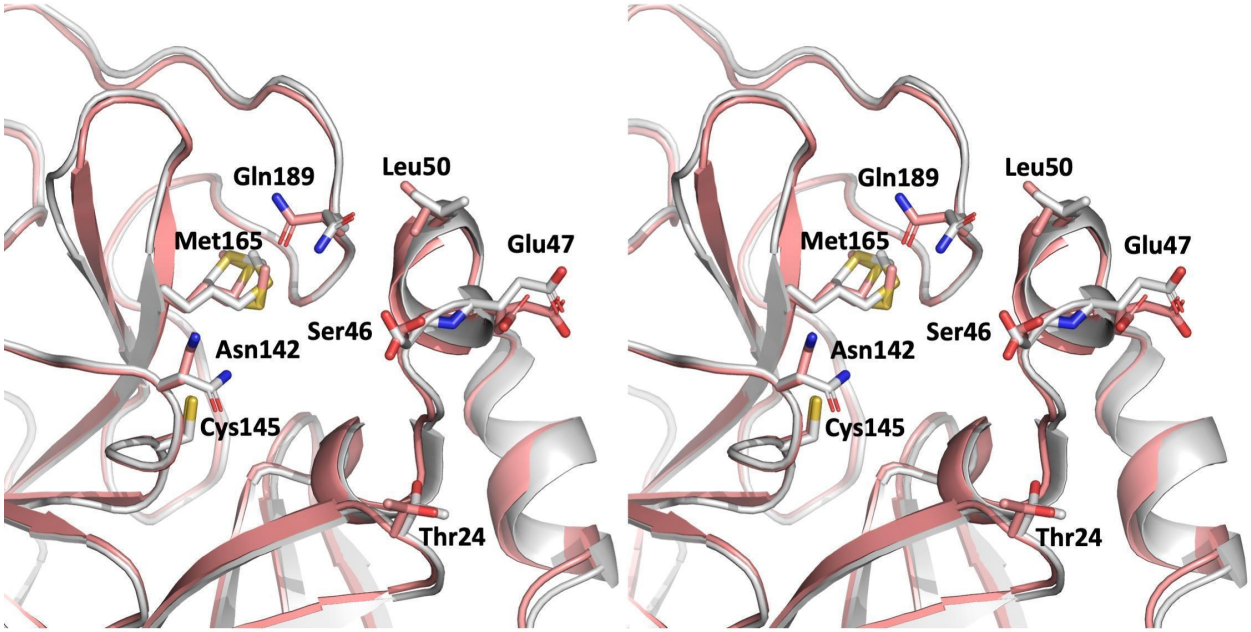

Figure S6 Wall-eye stereo image of the superposition of the active site of SFX structure (PDB ID: 7CWB) with ambient-temperature structure (PDB ID: 6WQF). Related to Figure 2.

Significant conformational states are observed at the putative inhibitor binding pocket. Residues with altered conformations were indicated by sticks, labeled and their positions were indicated. Our structure is colored in salmon while ambient-temperature structure (PDB ID: 6WQF) is colored in gray.

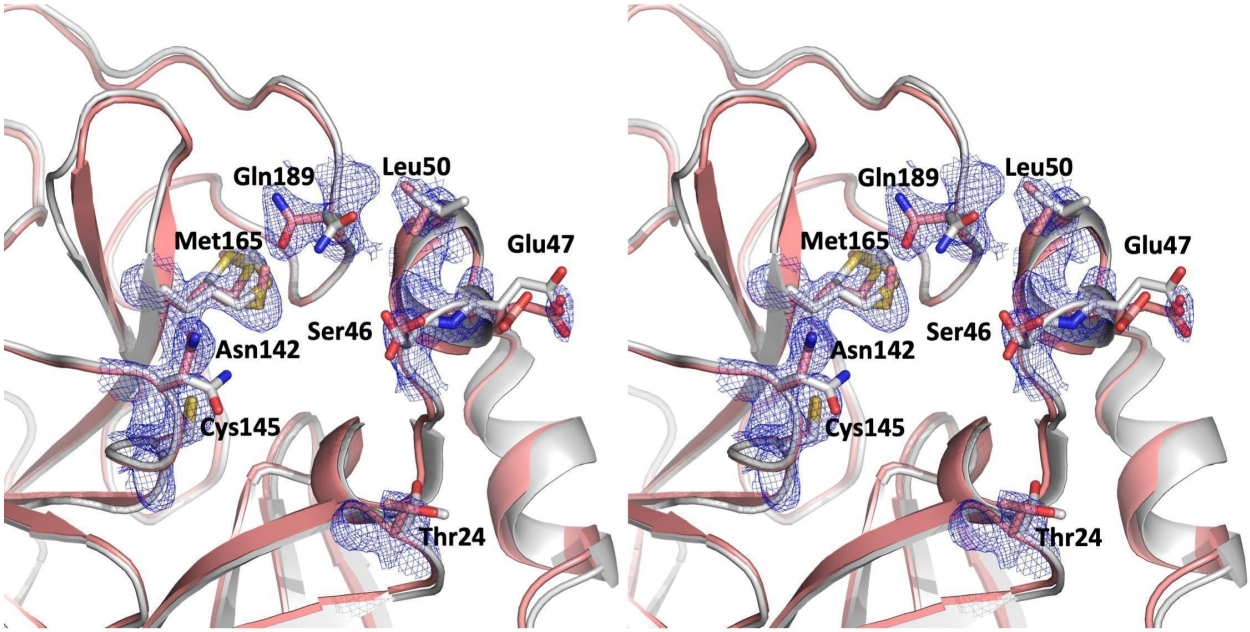

Figure S7 Wall-eye stereo image of composite omit electron density map of active site. Superposition the SFX structure (PDB ID: 7CWB) and ambient-temperature structure (PDB ID: 6WQF). Related to Figure 2.

The bias-free composite electron density belongs to residues with altered conformations of SARS-CoV-2 Mpro contoured at 1 sigma level and colored in slate. Our structure is colored in salmon while ambient-temperature structure (PDB ID: 6WQF) is colored in gray.

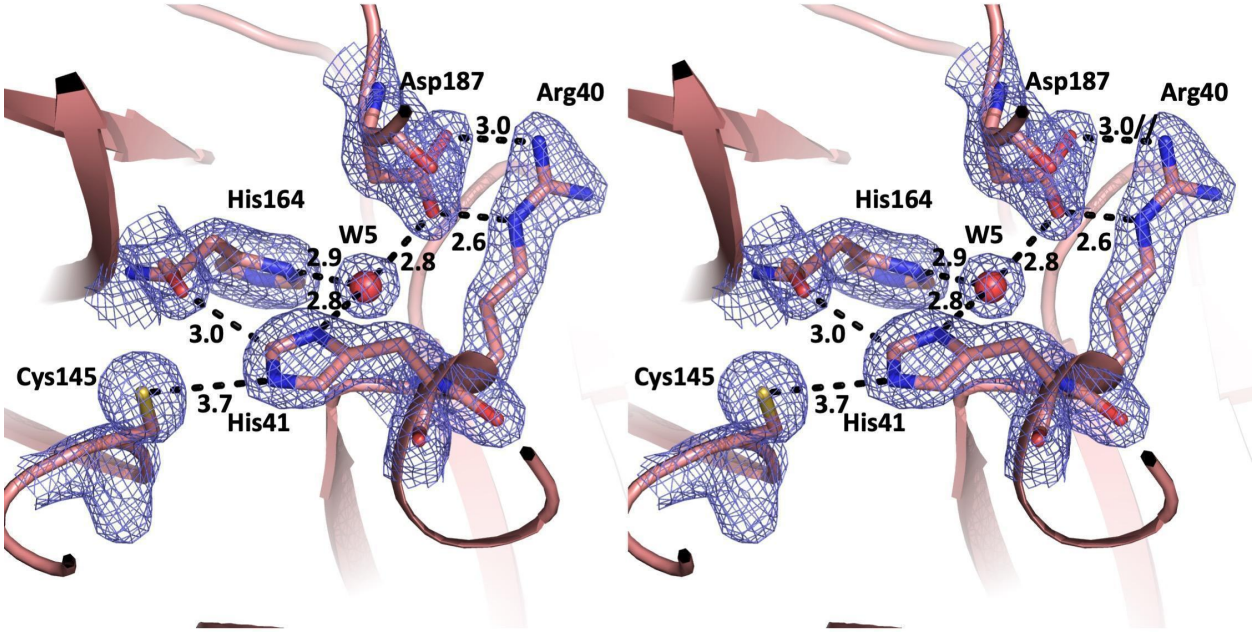

Figure S8 Wall-eye stereo image of SFX structure (PDB ID:7CWB) active site. Related to Figure 2.

2Fo-Fc electron density belonging to the active site residues are contoured in 1 sigma level and colored in slate. H-bonds and other interactions are indicated by dashed lines and distances are given by Angstrom.

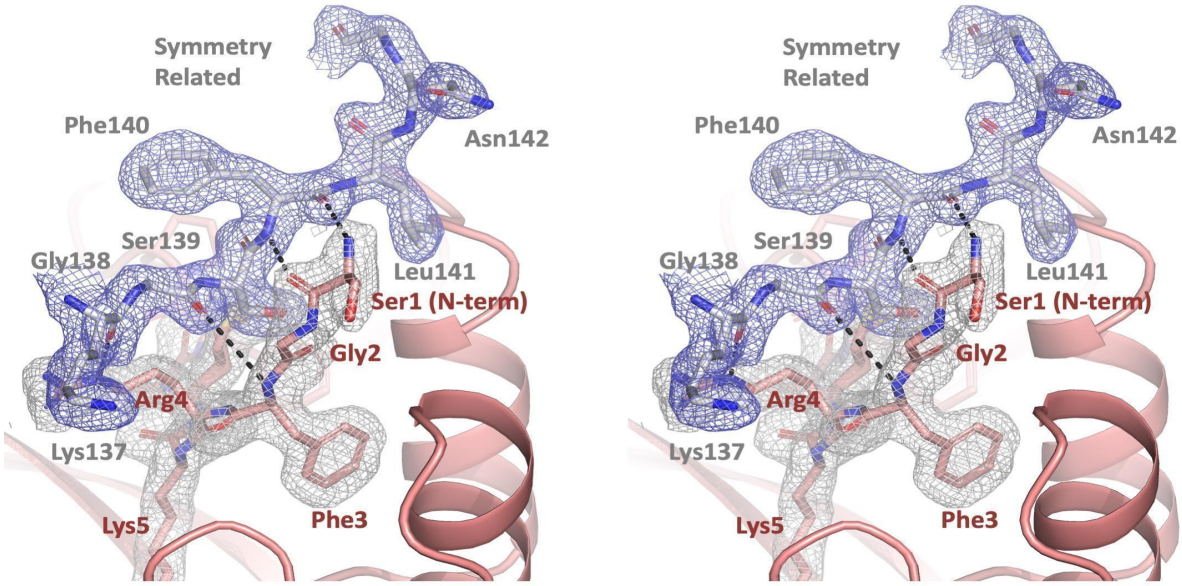

Figure S9 Wall-eye stereo image of key crystal contacts of C121 crystal form. Related to Figure 3.

The 2Fo-Fc electron density belongs to the N-terminal region of SARS-CoV-2 main protease contoured at 1 sigma level and colored in gray. Regions of the symmetry related molecule colored in gray, 2Fo-Fc electron density contoured in 1 sigma level and colored in slate. H-bonds are indicated by dashed lines. Elimination of these H-bonds were essential to obtain the second crystal form in $P2_12_12_1$ space group with more open inhibitor binding pocket for future soaking studies of the putative main protease inhibitors.

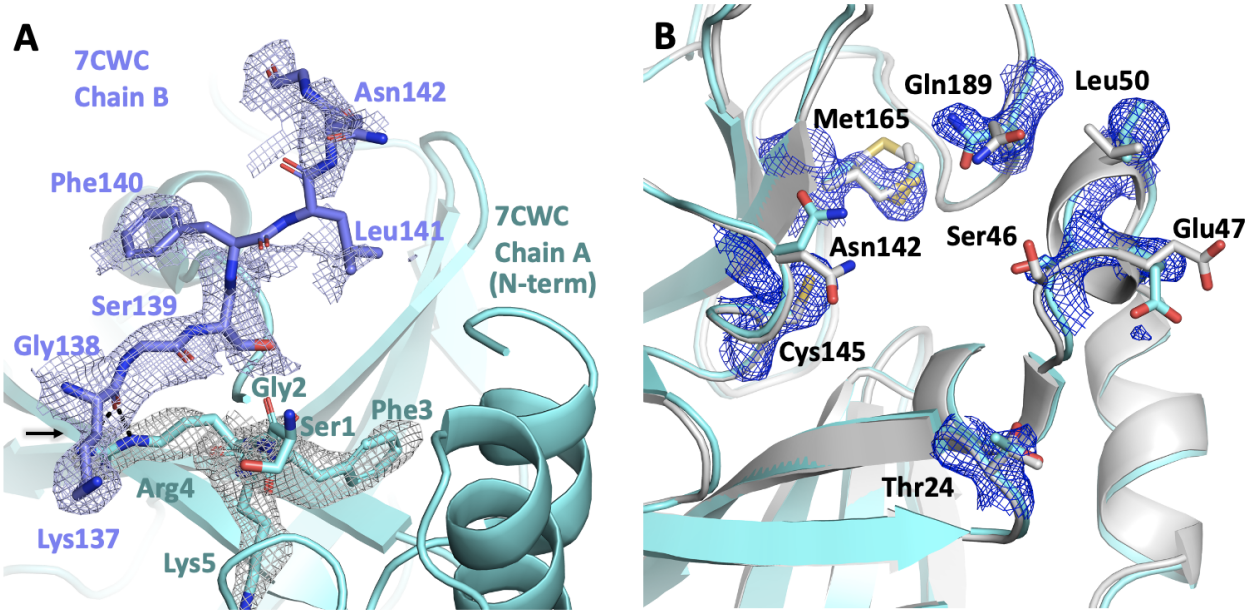

Figure S10 Key crystal contacts of P212121 crystal form. Related to Figure 3.

a) The 2Fo-Fc electron density belongs to the N-terminal region of SARS-CoV-2 main protease contoured at 1 sigma level and colored in gray. Region of the chain B is colored in gray, 2Fo-Fc electron density contoured in 1 sigma level and colored in slate. H-bonds are indicated by black dashed lines. Elimination of these H-bonds were essential to obtain the second crystal form in P212121 space group with a more open inhibitor binding pocket for future soaking studies of the putative main protease inhibitors. b) Superposition of our structure (PDB ID: 7CWC) is performed with Mpro structure (PDB ID: 6WQF). Our structure is colored with aquamarine while chain A of 6WQF is colored in gray. Composite omit map of 7CWC active site is shown in blue color.

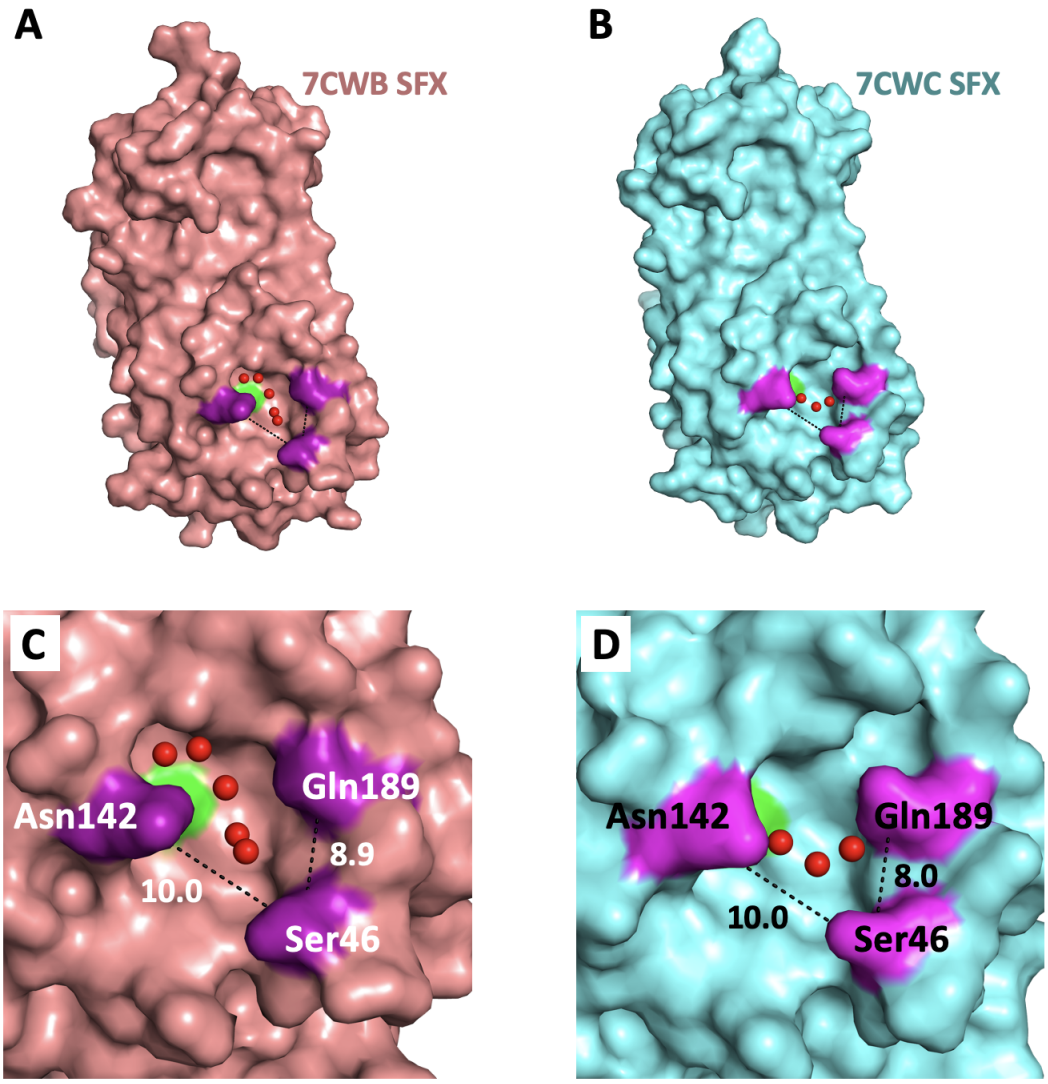

Figure S11 Different monoclinic crystal forms of the SARS-CoV-2 Mpro with catalytic site cavities. Related to Figure 6.

a) *C*121 SFX structure and **b)** chain A of $P2_12_12_1$ SFX structure. Water molecules in the catalytic cavity are shown with red spheres. The catalytic residue (Cys145) is highlighted in green and the flank cavity residues (Asn142, Ser46, Gln189) are highlighted in purple in the catalytic cavity of each crystal form **c)** *C*121 SFX and **d)** $P2_12_12_1$ SFX. Distance between C (Asn142 Cγ-Ser46 Cβ-Gln189 Cδ) atoms of flank cavity residues is shown as a dashed line. All distances are given in Angstrom (Å).

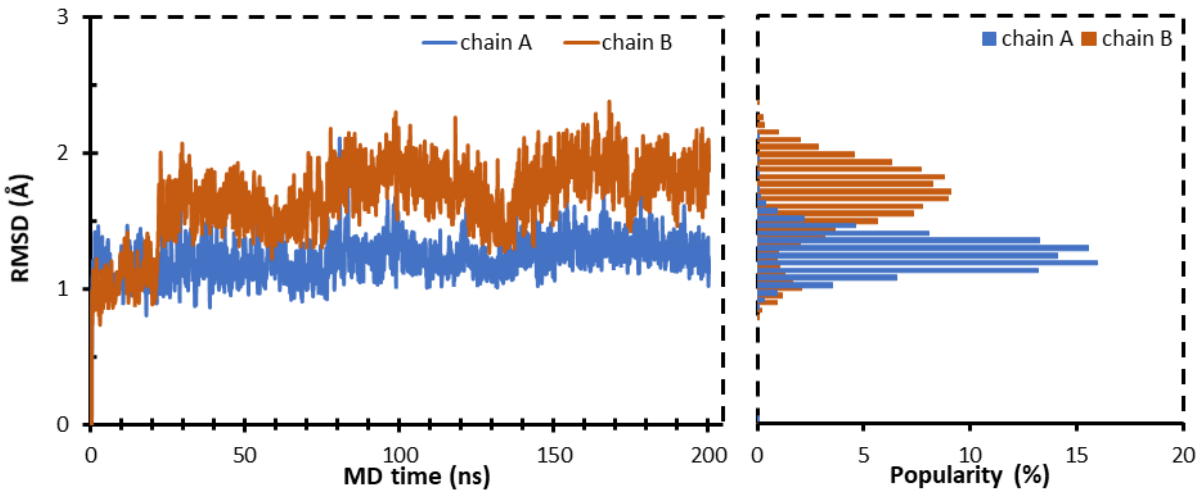

Figure S12 Changes in RMSD observed in Cα atoms during MD simulations with respect to initial trajectory frame for both chains of 7CWB. Related to Figure 4.

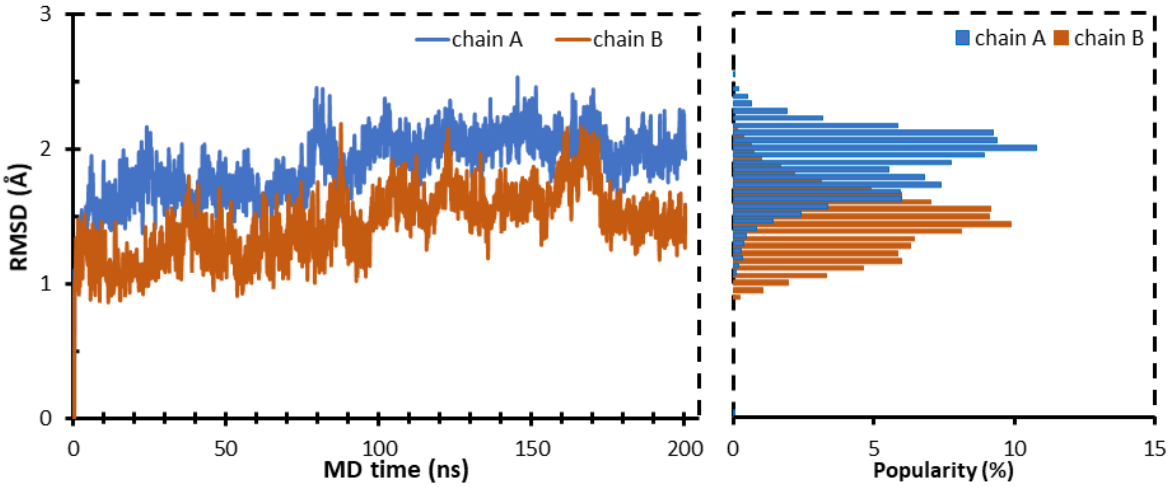

Figure S13 Changes in RMSD observed in Cα atoms during MD simulations with respect to initial trajectory frame for both chains of 7CWC. Related to Figure 4.

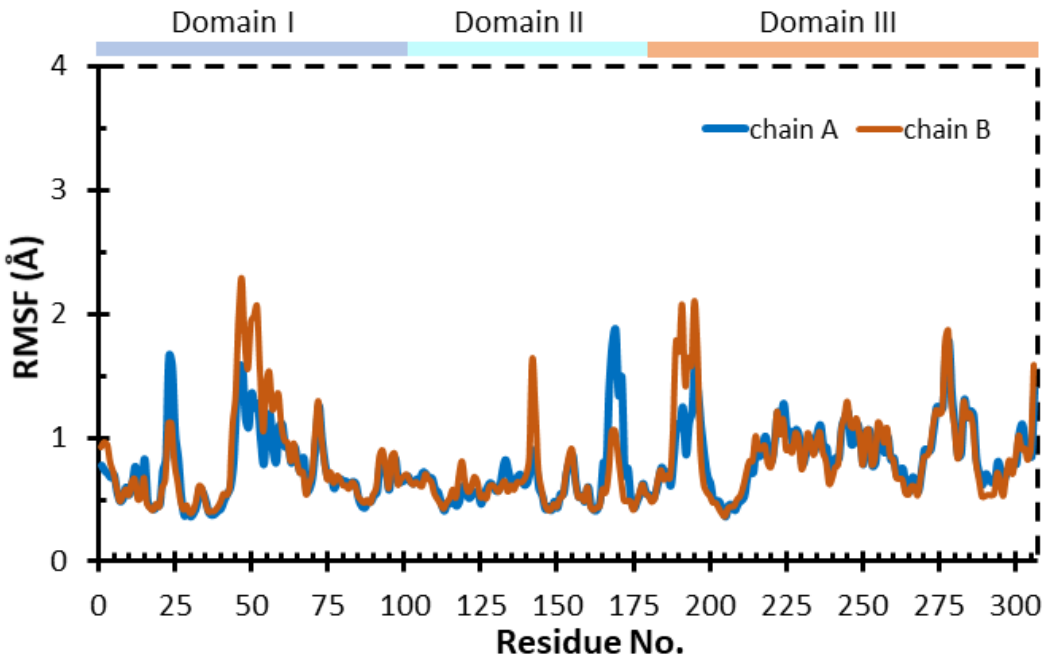

Figure S14 RMSF changes observed in Cα atoms during MD simulations for both chains of 7CWB with domains I, II and III also displayed above the graph. Related to Figure 4.

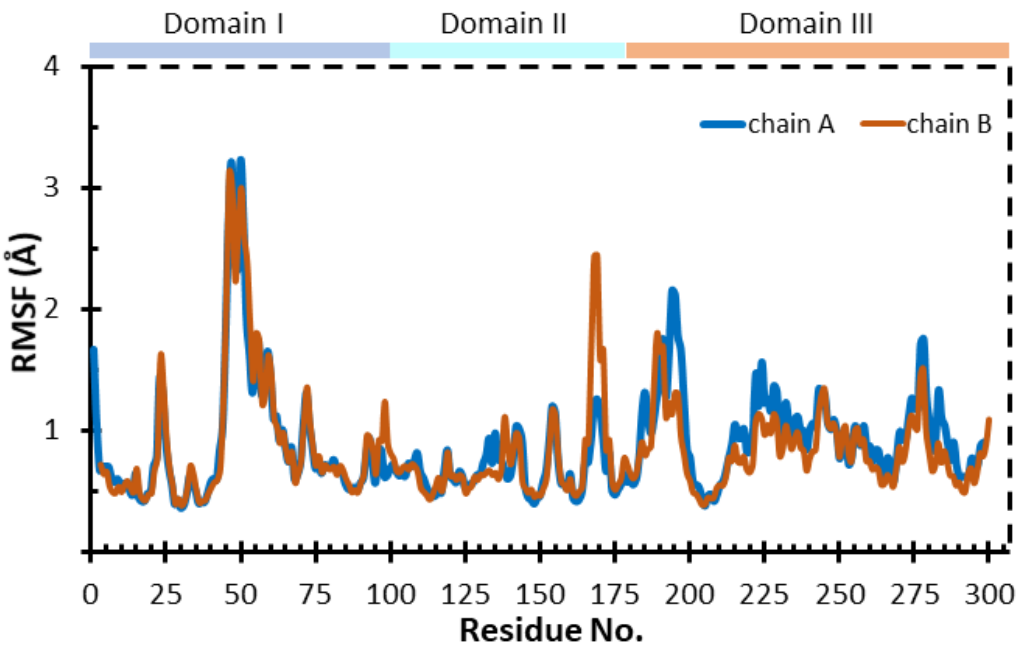

Figure S15 RMSF changes observed in Cα atoms during MD simulations for both chains of 7CWC with domains I, II and III also displayed above the graph. Related to Figure 4.

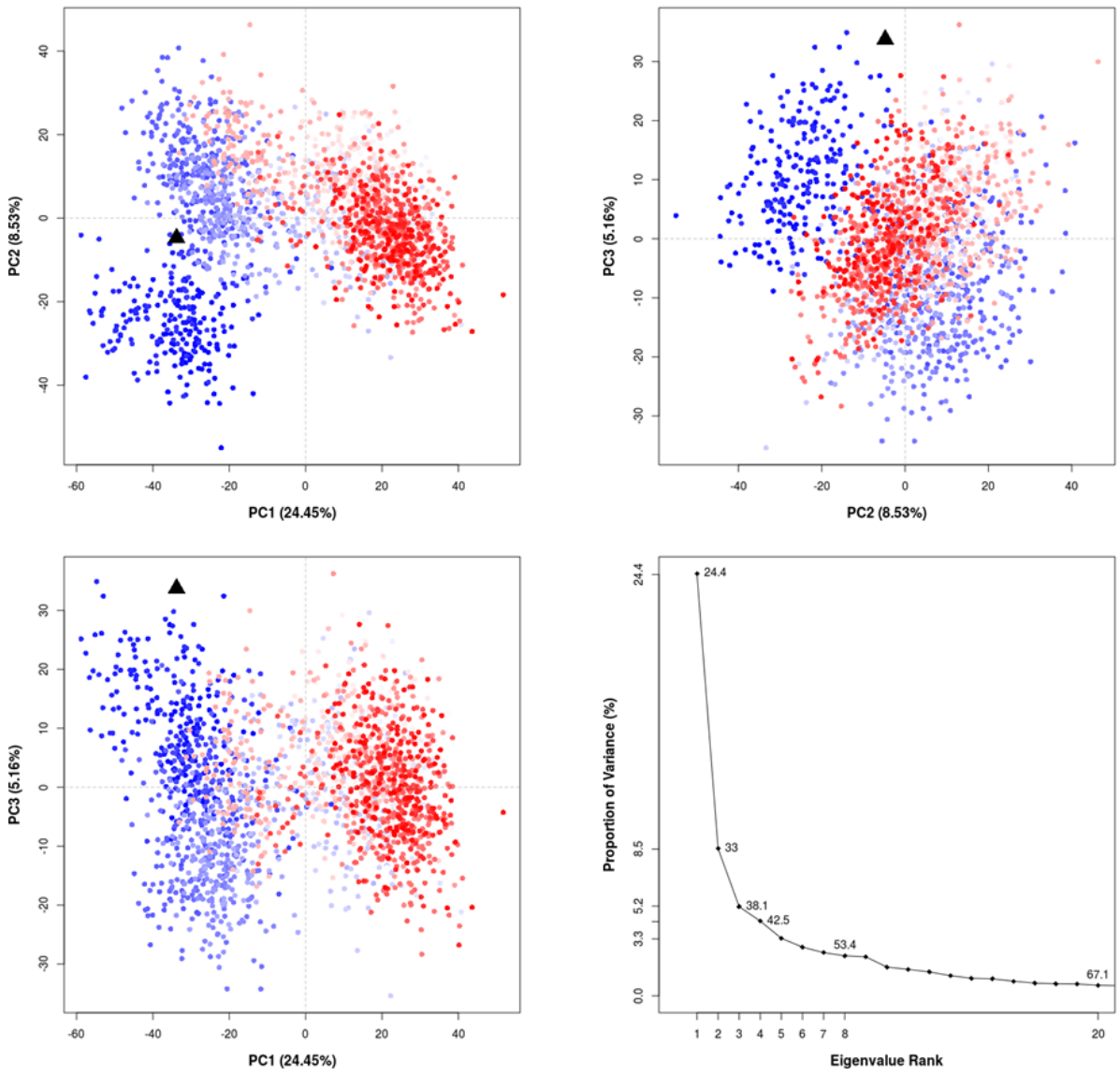

Figure S16 Projection of MD trajectory frames onto subspaces defined by the first three largest PCs as well as distribution of variance observed for eigenvalues for 7CWB. Related to Figure 4.

Instantaneous conformations (i.e. trajectory frames) colored from blue to red in order of trajectory time (200 ns). The black triangle represents the initial crystal structure conformation projected onto specified PCs.

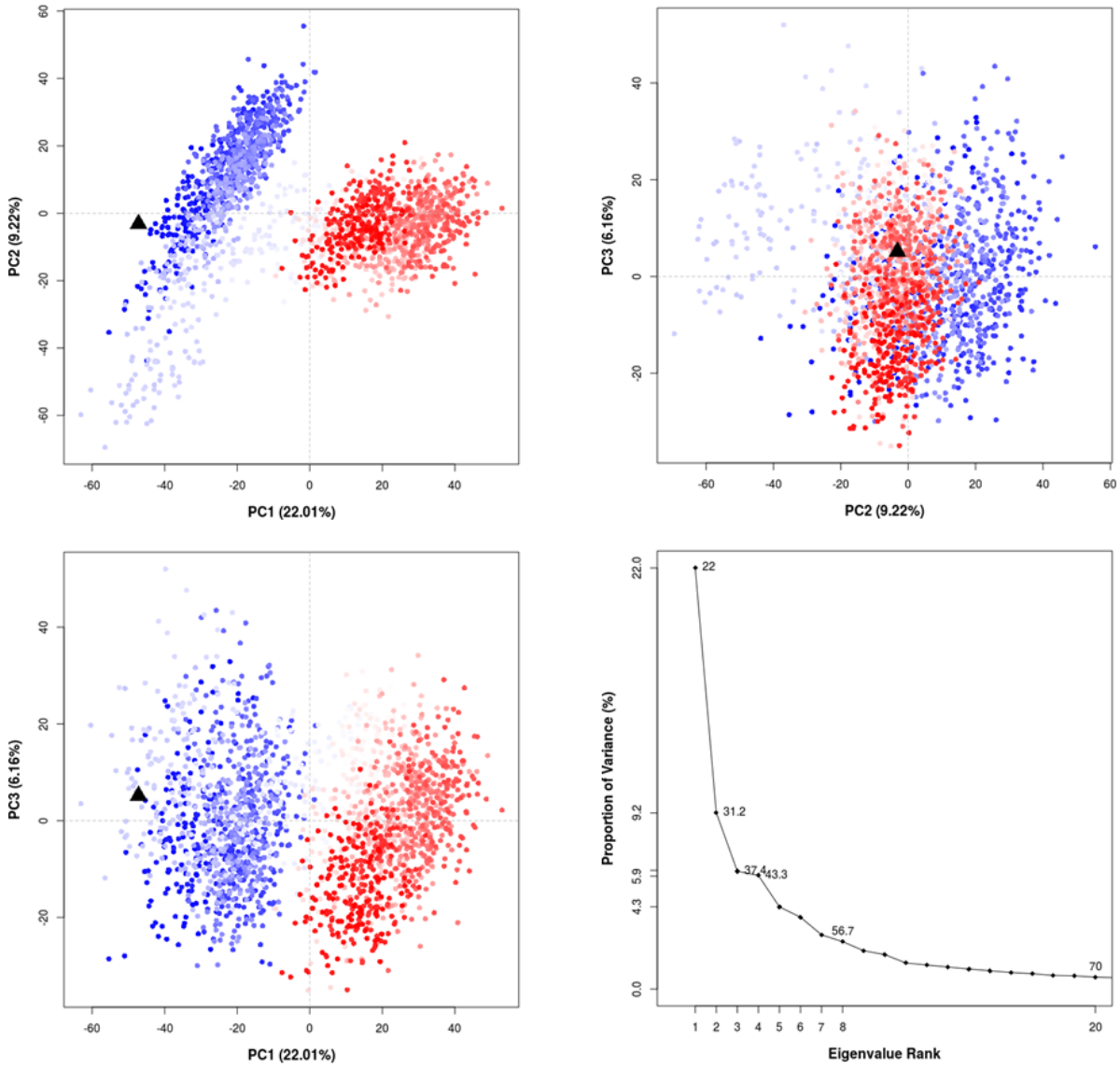

Figure S17 Projection of MD trajectory frames onto subspaces defined by the first three largest PCs as well as distribution of variance observed for eigenvalues for 7CWC. Related to Figure 4.

Instantaneous conformations (i.e. trajectory frames) colored from blue to red in order of trajectory time (200 ns). The black triangle represents the initial crystal structure conformation projected onto specified PCs.

Chain A	Chain B		6W63	6Y2E	6WQF	7C2Y	7CWB	7CWC
A:SER:1	B:PHE:140		0	0	0	0	1	0
A:SER:1	B:GLU:166		0	0	0	0	1	0
A:SER:1	B:HIS:172		0	0	0	0	1	0
A:GLY:2	B:SER:139		0	0	0	0	1	0
A:ARG:4	B:GLN:127		0	0	0	1	1	1
A:ARG:4	B:LYS:137		0	0	0	1	1	1
A:ARG:4	B:GLU:290		0	0	0	1	1	1
A:ALA:7	B:VAL:125		0	0	0	1	1	1
A:SER:10	B:SER:10		0	0	0	1	1	1
A:SER:10	B:GLU:14		0	0	0	1	1	1
A:GLY:11	B:GLU:14		0	0	0	1	1	1
A:GLU:14	B:SER:10		0	0	0	1	1	1
A:GLU:14	B:GLY:11		0	0	0	1	1	1
A:PRO:122	B:PHE:305		0	0	0	0	1	0
A:VAL:125	B:ALA:7		0	0	0	1	1	1
A:GLN:127	B:ARG:4		0	0	0	1	1	1
A:LYS:137	B:ARG:4		0	0	0	1	1	1
A:SER:139	B:GLY:2		0	0	0	0	1	0
A:SER:139	B:GLN:299		0	0	0	0	1	1
A:PHE:140	B:SER:1		0	0	0	0	1	0
A:GLU:166	B:SER:1		0	0	0	0	1	0
A:HIS:172	B:SER:1		0	0	0	0	1	0
A:GLU:290	B:ARG:4		0	0	0	1	1	1
A:GLN:299	B:SER:139		0	0	0	0	1	0
A:PHE:305	B:PRO:122		0	0	0	0	1	0

Figure S18 Comparison of the crystal structures of Mpro interfaces with respect to the H-bonds. Related to Figure 4 & 5

Domain I residues depicted in light blue, domain II and domain III depicted in pale cyan and dark salmon, respectively. Blue color shows hydrogen bonding, lines with red ones lack hydrogen bonding.

Chain A	Chain B		6W63	6Y2E	6WQF	7C2Y	7CWB	7CWC
A:ALA:116	B:MET:6		0	0	0	1	0	0
A:TYR:118	B:GLY:302		1	1	0	0	1	0
A:TYR:118	B:THR:304		1	0	1	0	1	0
A:SER:121	B:THR:304		1	1	1	0	1	0
A:SER:121	B:PHE:305		0	1	1	0	1	0
A:SER:121	B:GLN:306		0	1	0	0	0	0
A:PRO:122	B:PRO:9		1	1	1	1	1	1
A:PRO:122	B:THR:304		1	0	0	0	0	0
A:PRO:122	B:PHE:305		1	1	1	0	1	0
A:PRO:122	B:GLN:306		0	1	0	0	0	0
A:SER:123	B:PRO:9		0	0	0	1	0	0
A:SER:123	B:VAL:303		1	1	1	0	1	0
A:SER:123	B:THR:304		1	0	0	0	0	0
A:SER:123	B:PHE:305		1	1	1	0	1	0
A:GLY:124	B:MET:6		1	1	1	1	0	0
A:GLY:124	B:ALA:7		1	1	1	1	1	1
A:GLY:124	B:PRO:9		0	0	0	1	0	0
A:VAL:125	B:MET:6		0	1	0	0	1	1
A:VAL:125	B:ALA:7		1	1	1	1	1	1
A:VAL:125	B:PHE:8		1	0	1	0	1	0
A:VAL:125	B:VAL:125		1	1	1	1	1	1
A:TYR:126	B:ARG:4		0	0	1	1	1	1
A:TYR:126	B:LYS:5		1	0	0	0	0	0
A:TYR:126	B:MET:6		1	1	1	1	1	1
A:GLN:127	B:ARG:4		1	1	0	1	1	1
A:CYS:128	B:ARG:4		0	1	1	0	1	1
A:LYS:137	B:ARG:4		1	1	1	1	1	1
A:GLY:138	B:SER:1		1	0	0	0	0	0
A:GLY:138	B:GLY:2		1	1	1	0	1	0
A:GLY:138	B:ARG:4		0	0	0	0	1	0
A:SER:139	B:SER:1		1	1	1	0	1	0
A:SER:139	B:GLY:2		0	1	1	0	1	0
A:SER:139	B:MET:6		1	1	1	0	0	0
A:SER:139	B:GLN:299		1	1	1	0	1	1
A:PHE:140	B:SER:1		1	1	1	0	1	0
A:LEU:141	B:GLN:299		1	1	1	0	1	1
A:LEU:141	B:CYS:300		1	1	1	0	1	0
A:LEU:141	B:SER:301		1	0	1	0	1	0
A:LEU:141	B:GLY:302		1	1	1	0	1	0
A:GLU:166	B:SER:1		1	1	1	0	1	0
A:GLY:170	B:SER:1		1	0	0	0	0	0
A:HIS:172	B:SER:1		1	1	1	0	1	0

Figure S19 Evaluation of the crystal structures of Mpro interfaces with respect to the all possible interactions (salt bridges, pi-cation, pi-pi stacking, T-stacking, van der Waals (vdW), and H-bonds). Related to Figure 4 & 5.

Chain A	Chain B		7CWB	7CWC
A:TYR:118	B:GLY:302		63	0
A:TYR:118	B:THR:304		70	0
A:SER:121	B:THR:304		97	0
A:PRO:122	B:THR:304		86	0
A:PRO:122	B:PHE:305		99	0
A:SER:123	B:VAL:303		92	0
A:SER:123	B:PHE:305		84	0
A:GLY:124	B:ALA:7		99	97
A:VAL:125	B:MET:6		79	86
A:VAL:125	B:ALA:7		100	100
A:VAL:125	B:VAL:125		64	67
A:TYR:126	B:ARG:4		24	69
A:TYR:126	B:MET:6		78	73
A:GLN:127	B:ARG:4		32	69
A:CYS:128	B:ARG:4		45	61
A:LYS:137	B:ARG:4		94	1
A:GLY:138	B:PHE:3		2	97
A:SER:139	B:GLY:2		75	0
A:SER:139	B:PHE:3		77	83
A:SER:139	B:ARG:4		99	100
A:SER:139	B:GLN:299		64	8
A:PHE:140	B:SER:1		99	0
A:LEU:141	B:GLN:299		75	37
A:LEU:141	B:GLY:302		65	0
A:ASN:142	B:ARG:298		0	87
A:ASN:142	B:GLN:299		0	80
A:ASN:142	B:SER:301		0	83
A:GLU:166	B:SER:1		100	0

Figure S20 Dynamic valuation of the 7CWB and 7CWC dimer interfaces, all possible interactions were taken into account. Related to Figure 4.

Interaction propensity depicted as BWR color heatmap (interactions percentages were given respect to their conservation during the simulation.).

Chain A	Chain B		7CWB	7CWC
A:SER:1	B:PHE:140		100	0
A:SER:1	B:GLU:166		99	0
A:ARG:4	B:LYS:137		86	91
A:ARG:4	B:SER:139		75	36
A:ARG:4	B:GLU:290		100	100
A:ALA:7	B:VAL:125		100	100
A:SER:10	B:SER:10		100	100
A:GLY:11	B:GLU:14		100	100
A:GLU:14	B:GLY:11		80	100
A:PRO:122	B:PHE:305		99	0
A:SER:123	B:VAL:303		61	0
A:VAL:125	B:ALA:7		100	100
A:LYS:137	B:ARG:4		82	0
A:SER:139	B:ARG:4		92	99
A:PHE:140	B:SER:1		99	0
A:ASN:142	B:SER:301		0	67
A:GLU:166	B:SER:1		99	0
A:GLU:290	B:ARG:4		99	100
A:ARG:298	B:TYR:118		0	72
A:GLN:299	B:SER:139		16	65
A:PHE:305	B:PRO:122		98	0

Figure S21 Dynamic evaluation of dimer interfaces of 7CWB, and 7CWC. Only H-bonds were taken into account (0 shows no interaction was observed during MD simulations). Related to Figure 4.

Chain A	Chain B		7CWB	7CWC
A:GLY:283	B:LEU:286		23	75
A:LEU:286	B:GLY:283		27	64
A:LEU:286	B:ALA:285		52	62
A:GLU:290	B:ARG:4		100	100
A:ARG:298	B:TYR:118		0	72
A:GLN:299	B:SER:139		34	90
A:GLN:299	B:PHE:140		0	64
A:GLN:299	B:LEU:141		73	54
A:CYS:300	B:LEU:141		37	64
A:GLY:302	B:TYR:118		70	0
A:VAL:303	B:SER:123		84	0
A:THR:304	B:TYR:118		71	0
A:THR:304	B:SER:121		96	0
A:THR:304	B:PRO:122		84	0
A:PHE:305	B:PRO:122		99	0
A:PHE:305	B:SER:123		85	0

Figure S22 Dynamic evaluation of dimer interfaces of 7CWB, and 7CWC. All possible interactions were taken into account. Related to Figure 4.

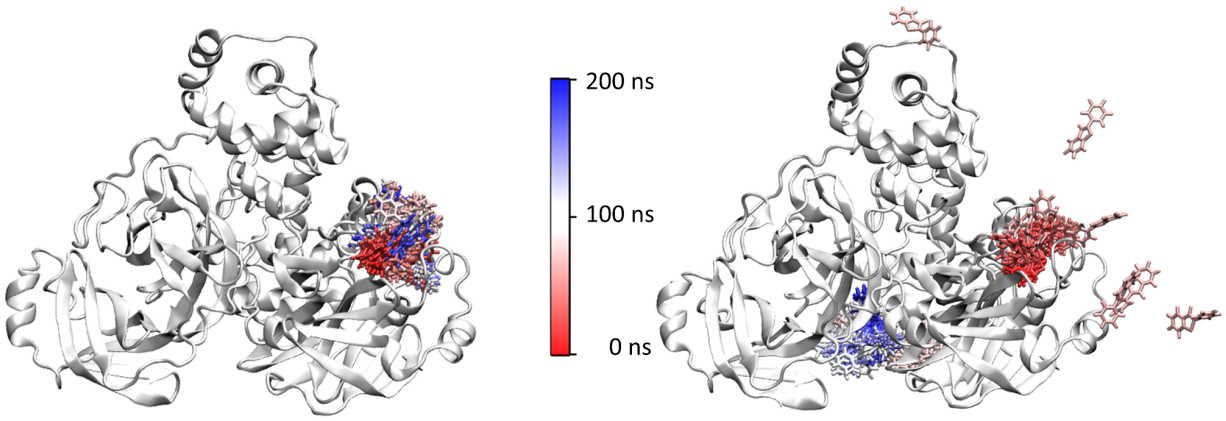

7CWC - Carmofur

7CWC - Ebselen

Figure S23 Binding poses of Carmofur (left) and Ebselen (right) at the 7CWC throughout the MD simulations. Related to Figure 5

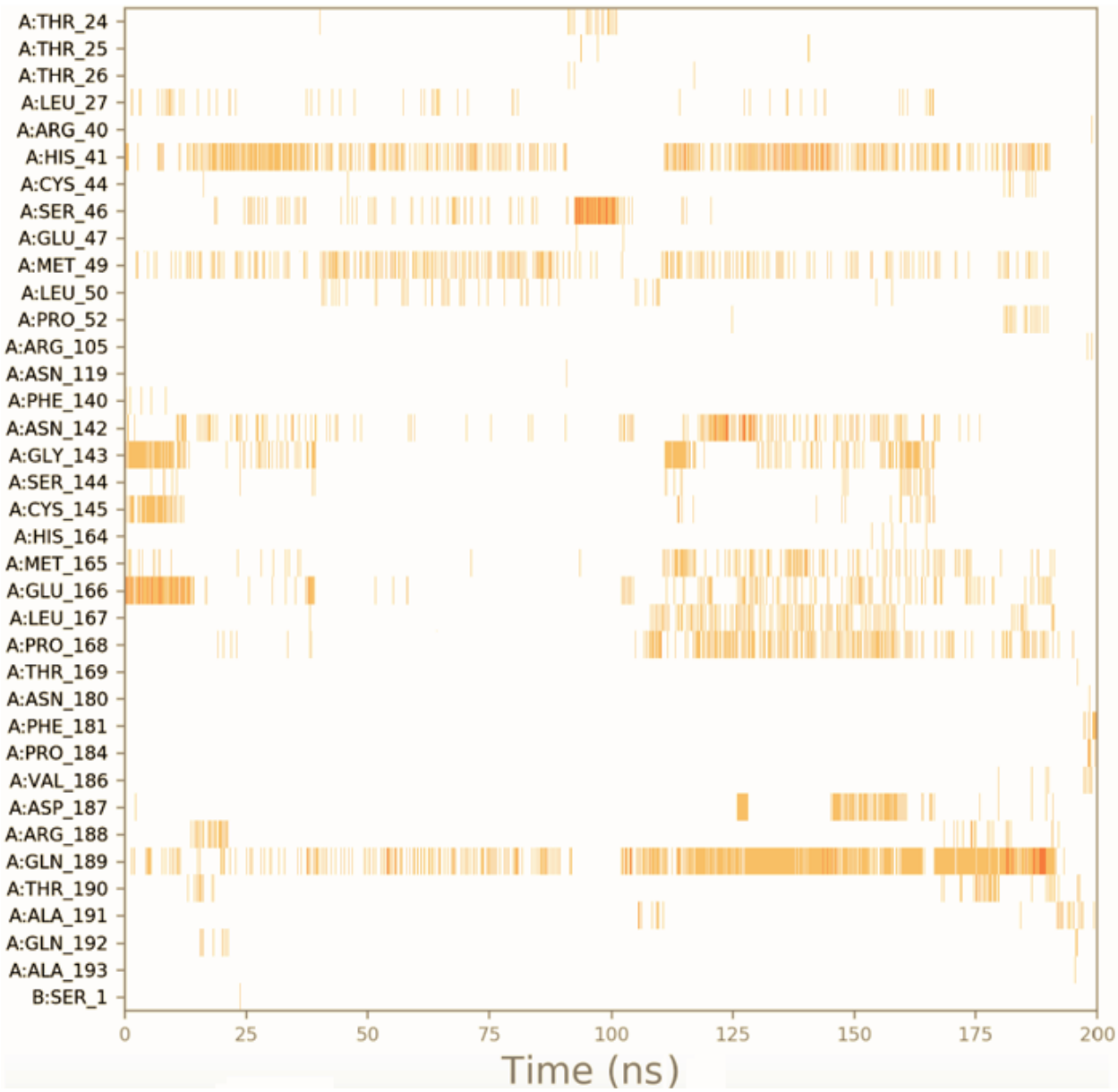

Figure S24 Timeline contacts of Tideglusib at the binding pocket of 6Y2E. Related to Figure 5.

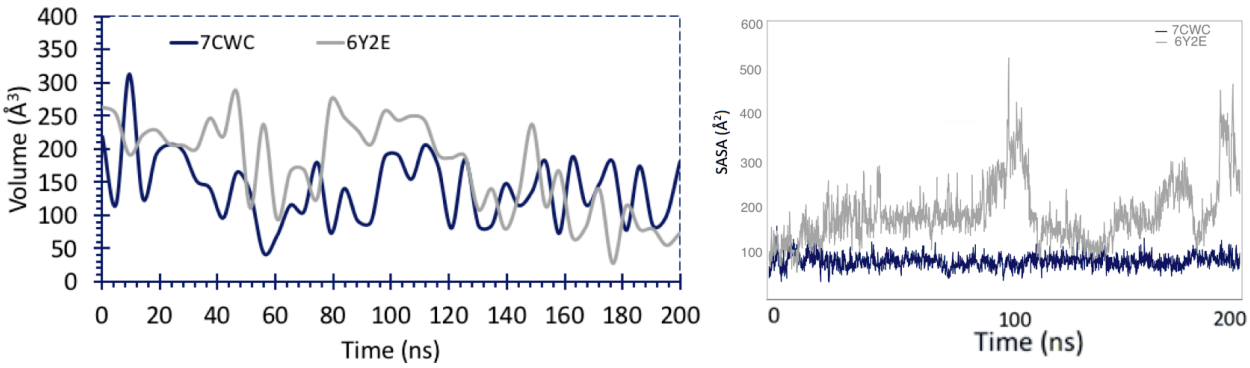

Figure S25 Binding pocket volume (left) and SASA (right) comparison of 7CWC and 6Y2E throughout the MD simulations of Tideglusib bound 7CWC and 6Y2E structures. Related to Figure 5.

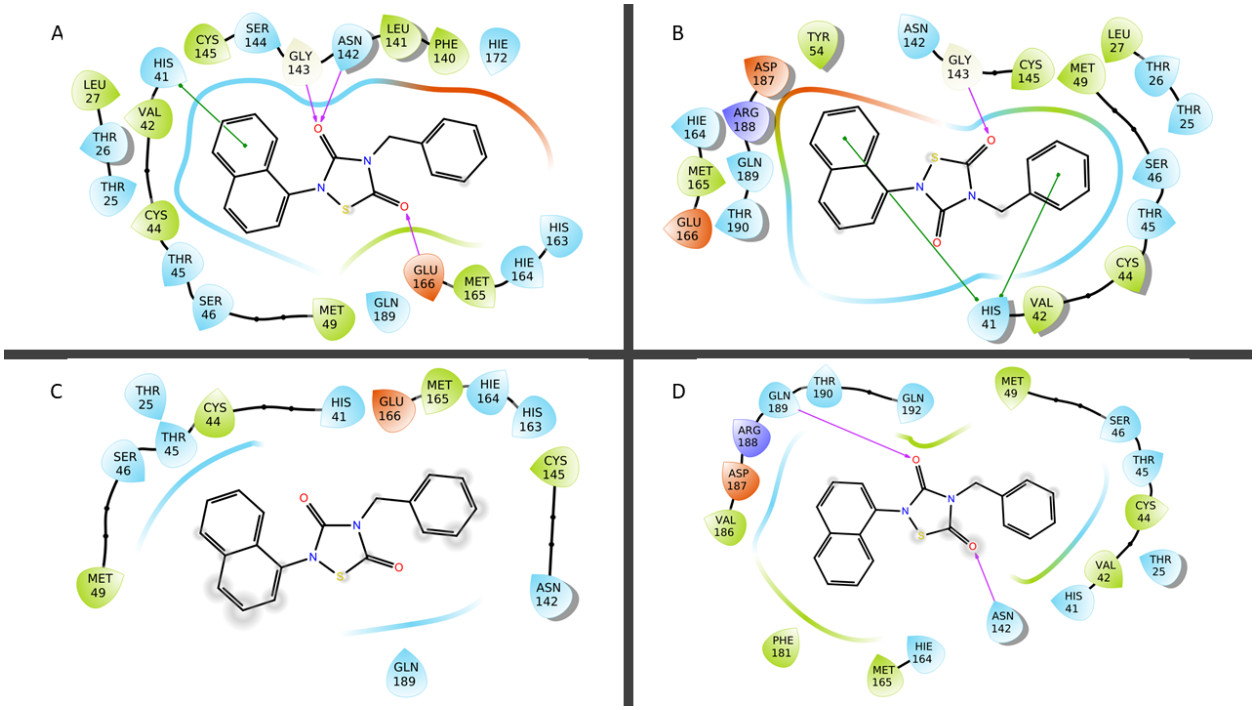

Figure S26 Comparison of the IFD poses of Tideglusib at the binding pocket of A) 7CWB and B) 6WQF. Related to Figure 5.

Representative poses that are obtained from MD simulations **C)** 7CWB and **D)** 6WQF.

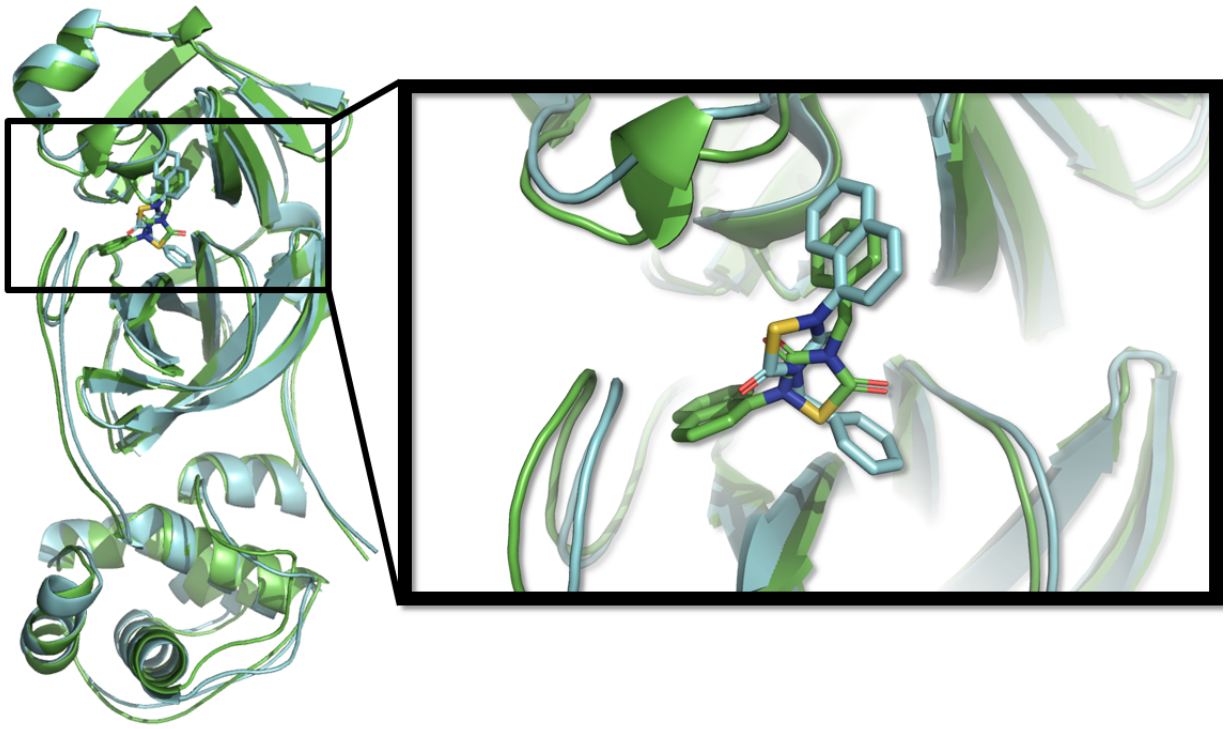

Figure S27 Alignment of the representative structures of Tideglusib complexes (7CWB, cyan, and 6WQF, green). Related to Figure 5.

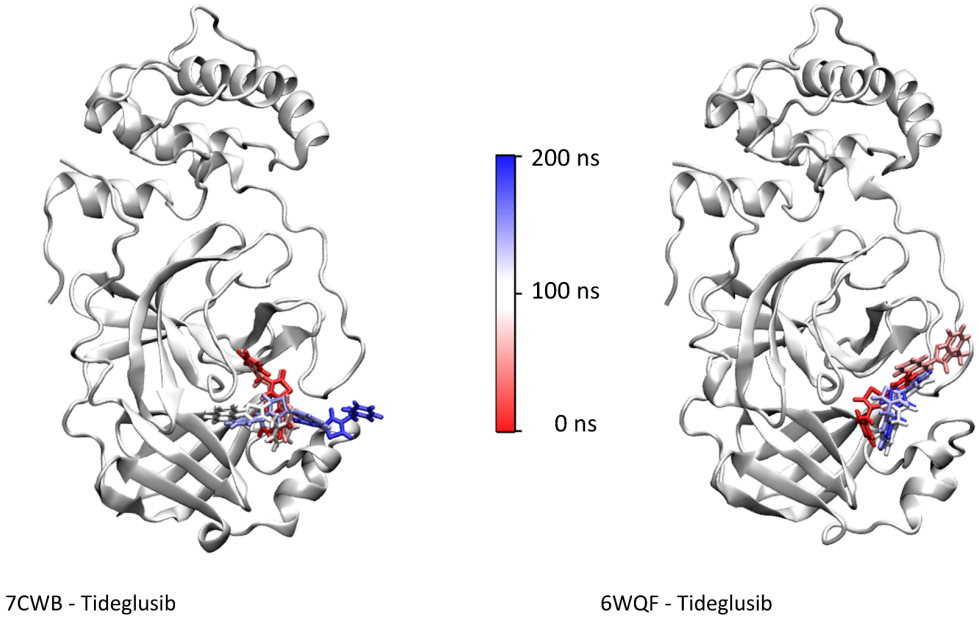

Figure S28 Tideglusib conformations explored during MD simulations on 7CWB (left) and 6WQF (right). Related to Figure 5.

Starting conformations and last frame depicted in red and blue color, respectively.

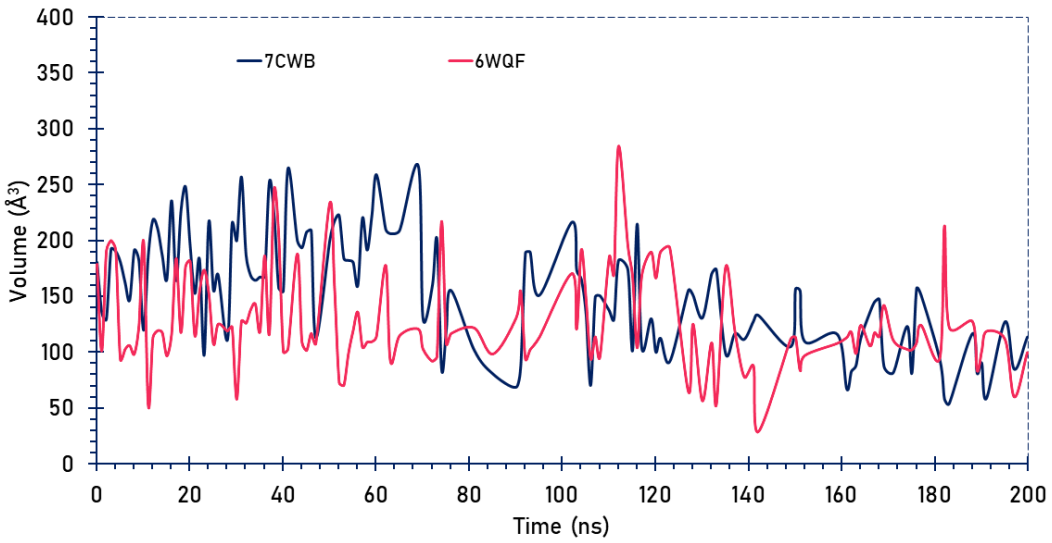

Figure S29 Binding pocket volume changes throughout the MD simulations. Related to Figure 5.

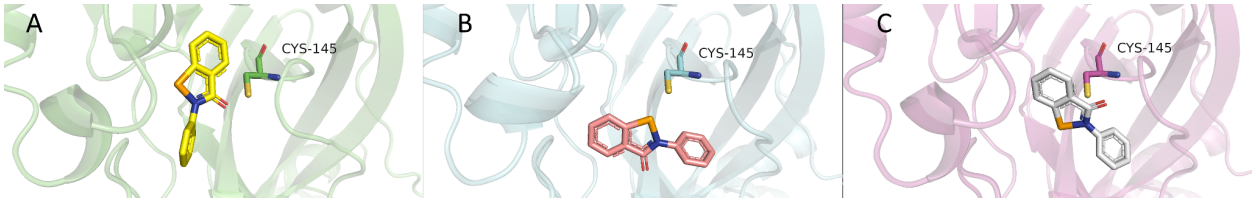

Figure S30. Ebselen binding poses at the active site of the MPro. Related to Figure 5.

Catalytic residue Cys145 depicted as sticks. Induced Fit Docking (IFD) poses of the Ebselen for the 7CWC (A), 6W63 (B), and 6Y2E (C), respectively. All of the poses are located very close to the Cys145 (in different orientations).

Supplementary Table S1 Data collection and refinement statistics for X-ray crystallography. Related to Figure 1.

Dataset	Monoclinic	Orthorhombic
PDB ID	7CWB	7CWC
Data collection[1]		
Beamline	LCLS (MFX)	LCLS (MFX)
Space group	C121	$P2_12_12_1$
Cell dimensions		
a, *b*, *c* (Å)	114.0, 53.5, 45.0	69.2, 104.3, 105.6
α, β, γ (°)	90, 102, 90	90, 90, 90
Resolution (Å)[2]	55.0-1.9 (1.98-1.90)[2]	75.0-2.1 (2.14-2.10)[2]
R_{split}	0.63 (0.94)	0.59 (3.33)
CC1/2	0.996 (0.598)	0.997 (0.634)
$I / \sigma I$	10.4 (0.57)	11.2 (0.33)
CC*	0.999 (0.865)	0.999 (0.678)
Completeness (%)	100.0 (100.0)	100.0 (100.0)
Redundancy	825 (266)	3105 (2025)
Refinement		
Resolution (Å)	34.0-1.9 (1.95-1.90)	42.0-2.1 (2.15-2.10)
No. reflections	21029 (1359)	45238 (3044)
R_{work} / R_{free}	0.22/0.26 (0.43/0.49)	0.22/0.26 (0.37/0.44)
No. atoms		
Protein	2447	4710
Ligand/Ion/Water	113	166
B-factors		
Protein	42.86	65.66
Ligand/Ion/Water	51.0	73.9
Coordinate errors	0.34	0.34
R.m.s deviations		
Bond lengths (Å)	0.007	0.003
Bond angles (°)	0.869	0.619
Ramachandran plot		
Favored (%)	294 (96.7)	580 (97.5)
Allowed (%)	9 (3.0)	14 (2.4)
Disallowed (%)	1 (0.3)	1 (0.1)

[1]Datasets are collected by serial crystallography.

[2]The highest resolution shell is shown in parenthesis.

Supplementary Table S2 SFX data collection statistics. Related to Figure 1.

Sample	Start Time	Stop Time	Total Run Time	Effective Run Time	Runs	Run Number	Total number frames collected	Total number frames with more than 30 Bragg reflections and a signal to noise ratio > 4.5	Total number of crystal lattices indexed to the appropriate unit cell	Total number of crystal lattices merged into the final SFX dataset
7CWB	10:17:31	13:16:48	2h 59m 17s	2h 47m 7s	118-141	34	1163413	208839	168655	160510
7CWC	10:49:37	12:40:36	1h 50m 59s	1h 36m 20s	320-339	20	686808	214355	157976	156512